RSC Advances

This is an *Accepted Manuscript*, which has been through the Royal Society of Chemistry peer review process and has been accepted for publication.

Accepted Manuscripts are published online shortly after acceptance, before technical editing, formatting and proof reading. Using this free service, authors can make their results available to the community, in citable form, before we publish the edited article. This *Accepted Manuscript* will be replaced by the edited, formatted and paginated article as soon as this is available.

You can find more information about *Accepted Manuscripts* in the **Information for Authors**.

Please note that technical editing may introduce minor changes to the text and/or graphics, which may alter content. The journal's standard **Terms & Conditions** and the **Ethical guidelines** still apply. In no event shall the Royal Society of Chemistry be held responsible for any errors or omissions in this *Accepted Manuscript* or any consequences arising from the use of any information it contains.

www.rsc.org/advances

Syntheses, crystal structures and properties of three cyano-bridged

one-dimensional coordination polymers based on macrocyclic metallic tectons

Xiang Jiang[&], Bo Tao[&], Xiaoli Yu, Yunhong Wang*, Hua Xia*

Faculty of Material Science and Chemistry, China University of Geosciences, Wuhan, 430074,

China

[&] *Both authors contributed equally to this work.*

* *Corresponding authors: 909098173@qq.com caihua223@gmail.com*

Three cyano-bridged nickel(II) complexes, namely, $[NiL_1][Ni(CN)_4] \cdot 3H_2O$ (**1**),

$[NiL_2][Ni(CN)_4] \cdot H_2O \cdot CH_3CN$ (**2**) and $[NiL_3][Ni(CN)_4] \cdot 3H_2O$ (**3**) (L_1=

1,3,6,8,11,14-hexaazatricyclo$[12.2.1.1^{8,11}]$octadecane, L_2=

1,3,6.8.12,15-hexaazatricyclo$[13.3.1.1^{8,12}]$eicosane and L_3=

1,3,6,9,11,14-hexaazatricyclo$[12.2.1.1^{6,9}]$octadecane) have been synthesized and characterized

based on different macrocyclic metallic tectons and diamagnetic $[Ni(CN)_4]^{2-}$. Single crystal X-ray

analyses reveal that complexes **1**-**3** exhibit a similar cyano-bridged one-dimensional chain

structure, in which one nickel(II) ion is coordinated by four nitrogen atoms from the macrocyclic

ligand and two nitrogen atoms from the bridging cyanide ligands, while the residual nickel(II) ion

is coordinated by four cyanide ligands. Interestingly, regulated by the peripheral macrocyclic

ligand, complex **1** features an unexpected large porous structure with the pore size of 1 nm, which

shows pronounced two steps adsorption of CO_2 gas at 195K. In additional, the magnetic properties

of complexes **1**-**3** show the presence of weak intrachain ferromagnetic interactions between the

paramagnetic nickel(II) ions through the diamagnetic $[Ni(CN)_4]^{2-}$ anions.

Introduction

Recent decades, considerable effort has been put on the rational construction of various dimensional (0D to 3D) porous coordination complexes (PCCs), which shows potential applications in gas adsorption and separation, catalysis and magnetism and so on[1-10]. Due to the success of reticular chemistry, porous frameworks featured three-dimensional structure, usually called metal-organic frameworks (MOFs) or porous coordination polymers (PCPs), are regard as the most rational ones to design and synthesis[11]. At the meantime, as shown by several groups, the generation of porous structures in 2D complexes is not a hard nut to crack because stacking of 2D layers (Kagome sheets for example) will produce some porous channel[12-15]. As for 0D porous complexes, a large number of papers have been published discussing the porous structures based on metal-organic polyhedrons and molecular cages since the end of last century[16-19]. On the contrary, progress on the formation of porous structures based on 1D coordination polymer has rarely been reported because of its dependency on the non-directional weak interactions (hydrogen bonds, π-π stacking *etc*) between 1D chains and an effective approach had not been proposed yet [20]. The rational control of the porous structure based on 1D coordination polymers remains largely unexplored thus far. Furthermore, it is also a huge challenge to obtain targeted organic porous framework based on infinite 1D chain in crystalline covalent organic frameworks (COFs), partial-ordered porous aromatic frameworks (PAFs) and disordered porous organic polymers (POPs). As same as porous coordination complexes, COFs, PAFs and POPs also can be built rationally to a 0D[21], 2D[22-23] and 3D[24-25] structures. However, we have not observed the pure organic framework from straight 1D chains yet (**note**: the basic structure of PIMs-polymers of intrinsic microporosity are not straight)[26]. Since PCCs are definite crystalline networks and their

precise structures can be easily determined through single-crystal X-ray diffraction analysis, PCCs

provide the most straightforward system in the study of porous materials based on 1D chains.

It has been realized that the 1D coordination polymers can easily be synthesized by linear

ligands coordinated to the univalent coinage-metal ions Ag(I)/Cu(I) as 2-connected nodes[27].

Recently, the macrocyclic complex had emerged as another smart node selection, because

macrocyclic complexes possess two residual potential coordination sites at axial positions. This

merit can be used to construct coordination polymers controllably. In fact, on the basis of this

considerations, Suh[28], Lu[29, 30], Jin[31], Kou[32] and other groups had fabricated several novel 1D

coordination polymers based on macrocyclic metallic precursors and organic carboxylic or

cyano-bridged ligands.

Herein, we present three cyano-bridged one-dimensional nickel(II) complexes based on

$[Ni(CN)_4]^{2-}$ and macrocylic metallic tectons (Scheme 1), namely, $[NiL_1][Ni(CN)_4]\cdot 3H_2O$ (**1**),

$[NiL_2][Ni(CN)_4]\cdot H_2O\cdot CH_3CN$ (**2**)   and $[NiL_3][Ni(CN)_4]\cdot 3H_2O$ (**3**)   (L_1=

1,3,6,8,11,14-hexaazatricyclo[12.2.1.1^{8,11}]octadecane, L_2=

1,3,6.8.12,15-hexaazatricyclo[13.3.1.1^{8,12}]eicosane   and L_3=

1,3,6,9,11,14-hexaazatricyclo[12.2.1.1^{6,9}]octadecane). The result indicates that the selection of

macrocylic ligands is clearly critical in determining their overall structures. Interestingly,

regulated by the structure of macrocyclic precursor, linear polymeric chains in the complex **1**

extend in three different directions generated by the 3-fold crystallographic axes to form an

unexpected one-dimensional porous structure. To the best of our knowledge this is the first work

that such 1D porous structure in complex **1** is observed among numerous $[Ni(CN)_4]^{2-}$ and

macrocylic metallic tectons related reports.

{Insert Scheme 1 here}

Materials and methods

Macrocyclic complexes $[NiL_1](ClO_4)_2$[33], $[NiL_2](ClO_4)_2$[33] and $[NiL_3](ClO_4)_2$[34] were prepared according to literatures. All other chemicals are commercially available and were used without further purification. The IR spectra were measured from KBr pellets on a Nicolet Avatar 370 FT-IR spectrometer. Elemental analyses were performed using a Vario ELIII CHNS/O elemental analyzer. Thermogravimetric analysis (TG) was performed on a Diamond TG-DTA 6300 equipment in flowing N_2 atmosphere with a heating rate of 10 °C min^{-1}. The powder X-ray diffraction measurements were performed on a Bruker D8 ADVANCE X-ray diffractometer. Sorption measurements for gases were measured with ASAP-2020M adsorption equipment. Desolvated samples were prepared under a dynamic vacuum ($<10^{-3}$ Torr) at 393 K for 10 h.

Caution! Perchlorate salts of metal complexes with organic ligands are potentially explosive. They should be handled with care and prepared only in small quantities in the synthesis of macrocyclic metallic tectons.

Synthesis of complexes 1-3

To a solution of $[NiL_{1-3}](ClO_4)_2$ (0.3 mmol) in 10 ml acetonitrile solution, a solution of $K_2[Ni(CN)_4]$ (0.72 g, 0.3 mmol) in 10 ml of aqueous solution was added with stirring, filtration and slow evaporation of the resulting solution gave crystals within three days. Yield: 60% (**1**), 15% (**2**) and 85% (**3**) based on $K_2[Ni(CN)_4]$. Anal. Calc. For **1**: C, 36.27; H, 6.09; N, 26.43%, found: C, 36.69; H, 5.90; N, 25.64%. For **2**: C, 42.77; H, 6.29; N, 27.45%, found: C, 42.80; H, 6.08; N, 28.02%. For **3**: C, 36.27; H, 6.09; N, 26.43%, found: C, 36.31; H, 6.02; N, 26.57%. IR, (**1**): 3494(s), 3224(s), 2917(s), 2871(s), 2148(s), 2123(s), 1635(s), 1488(m), 1453(m), 1336(m),

1287(w), 1097(s), 1025(m), 948(s), 844(s), 677(m). (**2**): 3441(s), 3240(s), 2921(s), 2857(s),

2148(s), 2124(s), 1640(w), 1461(m), 1370(m), 1333(m), 1271(m), 1100(m), 1080(s), 987(m),

950(m), 878(m), 805(m), 629(m), 564(w). (**3**): 3504(s), 3277(s), 2958(s), 2876(s), 2148(s),

2126(s), 1654(w), 1454(m), 1343(w), 1288(s), 1103(m), 978(w), 918(m), 707(m), 660(m).

Single-crystal X-ray data collection and structure determination

Single crystal X-ray diffraction data for complexes were collected on a Bruker Apex CCD

diffractmeter with graphite-monochromated Mo-Kα radiation ($\lambda = 0.71073$ Å) at 173(2) and 293(2)

K. Data reductions and absorption corrections were performed using the SAINT and SADABS

programs, respectively[35]. The structures were solved by direct methods using the SHELXS-97 or

SHELXS-2014 program and refined with full-matrix least squares on F^2 using the SHELXL-97 or

SHELXL-2014 program[36]. All the non-hydrogen atoms were refined anisotropically. The

hydrogen atoms were generated theoretically onto the specific atoms and refined isotropically with

fixed thermal factors. Since there is disorder of macrocyclic ligand in the complex **1**, they were

located and refined with restraints: DFIX, ISOR, SADI, SAME and EADP. Because of disordered

solvent molecules in complex **1**, the SQUEEZE routine of PLATON was used to remove the

diffraction contribution from these solvents to produce a set of solvent free diffraction

intensities[37]. Final formula of complex **1** was derived from crystallographic data combined with

elemental and thermogravimetric analysis data. The details of crystallographic data for the four

structures are summarized in Table 1, and the selected bond lengths and angles are listed in Table

S1.

{Insert Table 1 here}

Results and Discussion

Usually, the reaction rate of macrocyclic metallic precursors and $[Ni(CN)_4]^{2-}$ is extremely fast, the solution of macrocyclic complex and solution of $[Ni(CN)_4]^{2-}$ were mixed to produce a precipitate or microcrystalline powder immediately. However, it is worthwhile to note that the reaction of $[NiL_{1-3}](ClO_4)_2$ and $[Ni(CN)_4]^{2-}$ in CH_3CN and H_2O mixed solution give rise to a clear solution, generating the crystal of complexes **1-3** within three days. Compared to other macrocyclic metallic precursors, such as macrocyclic nickel complex containing 1,4,8,11-tetraazacyclotetradecane (cyclam) or 1,8-dimethyl-1,3,6,8,10,13-hexaazacyclotetradecane ligand[38], the slow reaction rate could be a result of the additional steric hindrance of side groups on macrocyclic ligand. In detail, compared with cyclam ligand, the addition of ethyl and propyl groups on L_{1-3} will slow down the formation of $Ni\cdots[Ni(CN)_4]^{2-}$ coordination bond. Further increase the steric hindrance on macrocyclic ligand may generate pure ionic compound according to the rule. This can be proved by introducing more complicated steric hindrance of the macrocyclic ligand as described in Kou's paper [39]. Hence, as a experimental rule, this merit can be utilized to fabricate more complicated cyano-bridged complexes based on macrocyclic metallic tectons $[NiL_{1-3}](ClO_4)$.

Single crystal X-ray analysis reveals that complexes **1-3** consist of one $[NiL_{1-3}]^{2+}$ cation, one $[Ni(CN)_4]^{2-}$ anion and several guest molecules (three water for **1**, one water and one acetonitrile for **2**, three water for **3**) (Figure 1a and Figure 2a). Different from the complexes **1** and **2**, the asymmetric unit of in complex **3** contains two parts of $[NiL_3]^{2+}$ (half $[Ni(1)L_3]^{2+}$, half $[Ni(2)L_3)]^{2+}$) (Figure 3a). In those complexes, one nickel ion coordinated by four cyanide ligands in a square planer geometry, the residual nickel ions surrounded by four nitrogen atoms from L_{1-3} ligand and two nitrogen atoms from two individual $[Ni(CN)_4]^{2-}$ anions with an octahedral geometry. Both

bond lengths and bond angles are in line with similar complexes (Table S1)[38]. Each $[Ni(CN)_4]^{2-}$

anion bridges two $[NiL_{1-3}]^{2+}$ fragments to generate a infinite 1D chain structure, whereas remains

two *trans* CN⁻ groups. The guest molecules occupy the vicinity of the chains and

hydrogen-bonded to the nitrogen atoms of mcrocyclic ligand and to each other. In complexes **2**

and **3**, all one-dimensional polymeric chains extend in one direction to form a close packing

structure (Figure 2b and Figure 3b). Unexpectedly and interestingly, the linear polymeric chains in

the **1** extend in three different directions generated by the 3-fold crystallographic axes to form a

one-dimensional porous structure with the pore size of 1 nm (Figure 1b, 1c). The void volume in

complex **1** is calculated by PLATON to be 25.4% of the total crystal volume[40]. Numerous papers

had been reported about the $[Ni(CN)_4]^{2-}$ bridged or even other cyanide-bridged one-dimensional

coordination polymers. The packing of one-dimensional chains usually occurs with a parallel

arrangement of all chains, such as in complex **2** and **3**, they can rarely extend along two different

directions[20], let alone in three different orientations. Furthermore, such type porous structure

appeared only once, a carboxylic-bridged one-dimensional coordination polymer based on

4,4'-diphenyldicarboxylic acid and macrocyclic metallic tecton $[Ni(cycalm)](ClO_4)_2$[41].

{Insert Figure 1 here}

Discussion of the structures

Complexes **1-3** are crystallized under the same environment (solvent and the ratio of raw

materials) apart from the different conformations of the macrocyclic ligands, which indicates that

their structural diversity in resulting complexes may be the result of the selection of macrocylic

ligands Such macrocylic ligand induced structure diversity maybe arises from four parts. 1) weak

Ni···Ni interaction. In complex **1**, the nearest interchain Ni···Ni distance from two $[Ni(CN)_4]^{2-}$ is

3.32 Å, which is short than the sum of *van der waals* radius[42], indicating the existence of a weak

Ni···Ni interaction. Due to the existence of such short Ni···Ni interaction, the 1-D [NiL$_1$][Ni(CN)$_4$]

chains point in three different directions, resulting a unexpected porous structure. Meanwhile, the

absence of short Ni···Ni interaction in complex **2** and **3** shows a common packing mode of their

1-D chains. 2) steric hindrance effect. Compared with the ethyl group on macrocyclic ligand L$_1$,

L$_2$ contains a propyl group. To a large extent, different groups will lead to different kinds of steric

hindrance effects in building the networks. 3) the symmetry of macrocyclic metallic tectons effect.

Two ethyl groups in the macrocyclic L$_1$ and two propyl groups in the macrocyclic L$_2$ were

arranged in a centro-symmetric position. On the contrary, in the L$_3$ ligand two ethyl groups were

located in the plane-symmetrical area. Seemingly, different symmetry may lead to a different

conformation of the macrocyclic ligand and thus to the resulting framework. 4) hydrongen bonding

interactions synergistic effect. Since the nature of hydrongen bond is non-directional and elusive,

combined with above three reasons, complexes **1-3** display entire different structures.

{Insert Figure 2 and 3 here}

IR spectral studies, thermogravimetric analyses and X-ray powder diffraction

The IR spectra show features attributable to the -CN triple bond stretching vibrations of the

complexes. The presence of split signals in the range of 2120-2150 cm^{-1} indicates the different

form of -CN on [Ni(CN)$_4$]$^{2-}$ (Figure S1). High frequency attributes the bridging mode and low

frequency correspond the vacant mode, which are consistent of crystal structure analyses. X-Ray

powder diffraction patterns of other complexes (Figure S2-S4) were recorded to confirm the purity

of the other as-synthesized bulk materials. The experimental XRD patterns match with the

calculated lines from the crystal structures. TGA shows that **1** loses all the free water molecules

and in the range of 30-100 °C (calculated: 10.92%, found: 11.00%) (Figure S5). The framework is

stable up to 260°C and then begins to decompose upon further heating. For **1**, the XRD pattern of

the activated sample solid (**1d**) is inconsistent with the simulated pattern, indicating the shrinkage

of the framework upon removal of guest molecules (Figure S2). When **1d** was immersed in the

mixture solution of water, the original framework of **1** was restored as evidenced by the PXRD

measurements (Figure S2).

Gas sorption properties of complex 1

To evaluate the porosity of **1d**, gas sorption studies were studied for N_2 (77K) and CO_2 (195K)

gases (Figure 4). Desolvated sample **1d** only shows very small N_2 sorption volume, however,

desolvated **1d** can adsorb CO_2, indicating that **1d** can selectively adsorb CO_2 over N_2. More

interestingly, the CO_2 sorption isotherm at 195 K measured up to 1 atm exhibits distinct two steps

in the adsorption process. The first step of adsorption should be related to the structure of **1d** with

shrunken pores, and the structure expands above the gate opening pressure to provide the second

step adsorption. It has been demonstrated that the multistep adsorption behaviors were related to

the structural transformations during the gas adsorption processes in macrocyclic complex based

porous coordination polymers[29]. This unusual behavior can be ascribed to the quadrupole

moment of CO_2 (-1.4×10^{-39}), which able to interact with the framework to open the channels.

From the adsorption data in the low range of P/P_0, the apparent Langmuir and

Brunauer-Emmett-Teller (BET) surface areas of the shrunken-pore phase of **1d** were estimated to

be 202.4 and 138.8 $cm^2 \cdot g^{-1}$ (Figure S6), respectively, and the pore volume estimated by the

Dubinin-Astakhov (DA) equation was 0.08 $cm^3 \cdot g^{-1}$. It is proved that, since the uptake amounts of

CO_2 gas in the whole desorption curve are much higher than adsorption, the expanded-pore phase

does not change back to the shrunken-pore phase of complex **1** during the desorption process. The

hysteretic behavior of CO_2 sorption can also be ascribed to the presence of interact between CO_2

molecules and **1d** framework.

{Insert Figure 4 here}

Magnetic properties of complexes 1-3

The variable-temperature magnetic susceptibility of complexes **1-3** were investigated at $H = 0.2$

T and $T = 2.0$-300 K. They are shown in the form of $\chi_m T$ versus T curve. As shown in Figure 5, the

$\chi_m T$ value is 0.957 emu K/mol (for **1**), 0.959 emu K/mol (for **2**) and 1.13 emu K/mol (for **3**) at

300K, which is close to the value of 1 emu K/mol expected for one spin-only Ni^{2+} ($3d^8$, $S=1$).

Curve fit of $1/\chi_m$ versus T for complexes **1-3** according to Curie-Weiss law $\chi_m = C/(T-\theta)$ gives C =

0.95 cm^3 K/mol, 0.96 cm^3 K/mol, 1.14 cm^3 K/mol and $\theta = 5.92$ K, 2.52 K, 1.32 K in temperature

range of 10-300 K, suggesting a weak ferromagnetic interaction between adjacent Ni^{2+} ions

(Figure S7-S9). As the temperature decrease, the $\chi_m T$ value increases very slowly and then sharply

fall to a minimum value of 0.52 emu K/mol (for **1**), 0.68 emu K/mol (for **2**) and 0.61 emu K/mol

(for **3**) at 2 K, which can be attributed to the presence of anti-ferromagnetic interaction between

one-dimensional chains. For the complexes **1-3**, the magnetic susceptibility can be expressed by

equation (1)[38, 43], where N is Avogadro's number, β is the Bohr magneton, k is the Boltzmann

constant and z is the number of nearest neighbors. The least-squares fitting to the experimental

data led to $J= 1.82$ (for **1**), 1.21 (for **2**) and 1.52 (for **3**), $zJ'= -1.78$ (for **1**), -1.13 (for **2**) and -1.60

(for **3**), g= 2.03 (for **1**), 2.09 (for **2**) and 2.15 (for **3**). This result of positive J shows the presence

of weak ferromagnetic interaction between the paramagnetic nickel ions within each chain through

the diamagnetic $[Ni(CN)_4]^{2-}$, and the negative zJ' shows the antiferromagnetic intermoleculer

interaction. The ferromagnetic coupling interaction can be explained by Goodenogh-Kanamori (G-K) rule[38]. According to G-K rule, if a magnetic orbital overlaps an empty orbital the interaction between the two ions is ferromagnetic. Adjacent magnetic nickel(II) ions contain unpaired d electrons can polarized on the empty d orbital of diamagnetic nickel(II) ion through the filled orbital of the cyanide bridges. Hence, it forms a ferromagnetic coupling.

$\chi_{chain}=Ng^2\beta^2/3KT\times(1+u)/(1-u)\times S(S+1)$

$u=cothK-1/K \text{ and } K=JS(S+1)/kT$

$\chi_m=\chi_{chain}/[1-\chi_{chain}(zJ'/Ng^2\beta^2)]$ Equation (1)

{Insert Figure 5 here}

Conclusion

In summary, under the consistent synthetic condition, three $[Ni(CN)_4]^{2-}$ involved structures have been presented based on macrocyclic metallic tectons. The comparisons of complexes indicate the slight difference between macocyclic ligands has a significant influence on their packing network. Unusual porous structure of complex **1** can adsorb CO_2 over N_2 molecules, suggesting that complex **1** is potential for the application of CO_2 separation. The magnetic measurements show the presence of weak intrachain ferromagnetic interactions between the paramagnetic nickel(II) ions through the diamagnetic $[Ni(CN)_4]^{2-}$ anions. The serendipity of complex **1** will provide some cue for those groups engaged in the porous organic polymers and porous inorganic-organic hybrid polymers.

Supplementary data

CCDC-1038632 (for **1**), 1038633 (for **2**) and 1038634 (for **3**) contain the supplementary

crystallographic data for this paper. These date can be obtained free of charge from The

Cambridge Crystallographic Data Centre viawww.ccdc.cam.ac.uk/data_request/cif.

Acknowledgements

References

[1]   A. Schneemann, V. Bon, I. Schwedler, I. Senkovska, S. Kaskel and R. A. Fischer, *Chem. Soc. Rev.*, 2014, **43**, 6062

[2]   G. Ferey, *Chem. Soc. Rev.*, 2008, **37**, 191

[3]   J. Y. Lee, O. K. Farha, J. Roberts, K. A. Scheidt, S. T. Nguyen and J. T. Hupp, *Chem. Soc. Rev.*, 2009, **38**, 1450

[4]   J.-R. Li, R. J. Kuppler and H.-C. Zhou, *Chem. Soc. Rev.*, 2009, **38**, 1477

[5]   L. E. Kreno, K. Leong, O. K. Farha, M. Allendorf, R. P. V. Duyne and J. T. Hupp, *Chem. Rev.*, 2012, **112**, 1105

[6]   J.-P. Zhang, Y.-B. Zhang, J.-B. Lin and X.-M. Chen, *Chem. Rev.*, 2012, **112**, 1001

[7]   M. P. Suh, H. J. Park, T. K. Prasad and D. W. Lim, *Chem. Rev.*, 2012, **112**, 782

[8]   H. N. Miras, L. vilà-Nadal and L. Cronin, *Chem. Soc. Rev.*, 2014, **43**, 5679

[9]   Q. P. Li, X. Jiang and S. W. Du, *RSC Adv.*, 2015,**5**, 1785

[10]   S. Furukawa, J. Reboul, S. Diring, K. Sumida and S. Kitagawa, *Chem. Soc. Rev.*, 2014, **43**,

5700

[11]   N. W. Ockwig, O. Delgado-Friedrichs, M. O'Keeffe and O. M. Yaghi, *Acc. Chem. Res.*, 2005, **38**, 176

[12]   X. Jiang, Z. Li, Y. Zhai, G. Yan, H. Xia and Z. Li, *CrystEngComm*, 2014, 16, 805

[13]   X.-R. Meng, D.-C. Zhong, L. Jiang, H.-Y. Li and T.-B. Lu, *Cryst. Growth Des.*, 2011, 11, 2020

[14]   M. P. Suh, H. J. Choi, S. M. So and B. M. Kim, *Inorg. Chem.*, 2003, **42**, 676

[15]   L. Jiang, X.-R. Meng, H. Xiang, P. Ju, D.-C. Zhong and T.-B. Lu, *Inorg. Chem.*, 2012,**51**, 1874

[16]   D. J. Tranchemontagne, Z. Ni, M. O'Keeffe and O. M. Yaghi, *Angew. Chem., Int. Ed.*, 2008, **47**, 5136

[17]   J. F. Eubank, H. Mouttaki, A. J. Cairns, Y. Belmabkhout, L. Wojtas, R. Luebke, M. Alkordi and M. Eddaoudi, *J. Am. Chem. Soc.*, 2011, **133**, 14204

[18]   Y. L. Liu, V. C. Kravtsov, D. A. Beauchamp, J. F. Eubank and M. Eddaoudi, *J. Am. Chem. Soc.*, 2005, **127**, 7266

[19]   M. Eddaoudi, J. Kim, J. B. Wachter, H. K. Chae, M. O'Keeffe and O. M. Yaghi, *J. Am. Chem. Soc.*, 2001, **123,** 4368

[20]   W. L. Leong and J. J. Vittal, *Chem. Rev.*, 2011, **111**, 688

[21]   G. Zhang, O. Presly, F. White, I. M. Oppel and M. Mastalerz, *Angew. Chem., Int. Ed.*, 2014, **126**, 1516

[22]   A. P. Côté, A. I. Benin, N. W. Ockwig, M. O'Keeffe, A. J. Matzger and O. M. Yaghi, *Science*, 2005, **310**, 1166

[23] Y. H. Xu, S. B. Jin, H. Xu, A. Nagai and D. L. Jiang, *Chem. Soc. Rev.*, 2013, **42**, 8012

[24] H. M. El-Kaderi, J. R. Hunt, J. L. Mendoza-Cortes, A. P. Cote, R. E. Taylor, M. O'Keeffe and O. M. Yaghi, *Science*, 2007, **316**, 268

[25] Y. Zhang, J. Su, H. Furukawa, Y. Yun, F. Gándara, A. Duong, X. Zou and O. M. Yaghi, *J. Am. Chem. Soc.*, 2013, **135**, 16336

[26] N. B. McKeown and P. M. Budd, *Chem. Soc. Rev.*, 2006, **35**, 675

[27] L. Carlucci, G. Ciani and D. M. Proserpio, *Coord. Chem. Rev.*, 2003, **246**, 247

[28] H. J. Choi and M. P. Suh, *J. Am. Chem. Soc.*, 1998, **120**, 10622

[29] P. Ju, L. Jiang and T. Lu, *Chem. Commun.*, 2013, **49**, 1820

[30] G.-C. Ou, L. Jiang, X.-L. Feng and T.-B. Lu, *Inorg. Chem.*, 2008, **47**, 2710

[31] S. L. Huang and G. X. Jin, *CrystEngComm*, 2011, **13**, 6013

[32] Z.-H. Ni, H.-Z. Kou, H.-Y. Zhao, L. Zheng, R.-J. Wang, A.-L. Cui and O. Sato, *Inorg. Chem.*, 2005, **44**, 2050

[33] M. P. Suh, S. G. Kang, V. L. Gocdken and S. Park, *Inorg. Chem.*, 1991, **30**, 365

[34] M. P. Suh, W. Shin, S.-G. Kang, M. S. Lah and T.-M. Chung, *Inorg. Chem.*, 1989, **28**, 1602

[35] *SMART, and SADABS*, Bruker AXS Inc.: Madison, Wisconsin, USA.

[36] G. M. Sheldrick, *Acta Crystallogr., Sect. A: Found. Crystallogr.*, 2008, **64**, 112.

[37] A. L Spek, PLATON, A Multipurpose Crystallographic Tool, Utrecht University, The Netherlands, 2006.

[38] Kou, H. Z.; Si, S. F.; Gao, S.; Liao, D. Z.; Jiang, Z. H.; Yan, S. P.; Fan,Y. G.; Wang, G. L. *Eur. J. Inorg. Chem.* 2002, **3**, 699

[39] H. Z. Kou, W. M. Bu, S. Gao, D. Z. Liao, Z. H. Jiang, S. P. Yan, Y. G. Fan and G. L. Wang, *J.*

Chem. Soc., Dalton Trans., 2000, 2996

[40] A. L. Spek, *J. Appl. Crystallogr.*, 2003, **36**, 7

[41] E. Y. Lee and M. P. Suh, *Angew. Chem., Int. Ed.*, 2004, **43**, 2798

[42] J.E. Huheey, Inorganic chemistry: principles of structure and reactivity (thirded) Harper &

Row Publishers, New York (1983)

[43] O. Kahn, Molecular Magnetism, VCH, Weinheim, Germany, 1993, Chapter 11, pp 257-258

Table 1. Crystallographic Parameters of Complexes **1-3**

	1	**2**	**3**
Space group	R-3c	P21/n	P-1
Temperature (K)	173(2)	293(2)	293(2)
a (Å)	28.9962(9)	9.812(2)	8.6927(17)
b (Å)	28.9962(9)	13.179(3)	9.6891(19)
C (Å)	32.8782(16)	20.122(4)	14.739(3)
α (°)	90	90	100.47(3)
β (°)	90	102.78(3)	93.41(3)
γ (°)□	120	90	110.83(3)
Volume (Å^3)	23939.8(16)	2537.6(10)	1130.5(5)
Z	36	4	2
GOF	1.04	1.17	1.09
Final R indices [I>2sigma(I)]	$R_1 = 0.0516$	$R_1 = 0.0721$,	$R_1 = 0.0462$
R indices (all data)	$wR_2 = 0.1429$	$wR_2 = 0.1978$	$wR_2 = 0.1246$

$GOF = [\Sigma w(F_o{}^2 - F_c{}^2)^2/(n_{obc} - n_{param})]^{1/2}$; $R_1 = ||F_o|-|F_c||/\Sigma|F_o|$, $wR_2 = [\Sigma w(F_o{}^2 - F_c{}^2)^2/\Sigma w(F_o{}^2)^2]^{1/2}$

16

Captions for the Figures:

Scheme 1. Macrocyclic metallic tectons.

Figure 1. (a) ORTEP figure of **1**, (b) view down the *c*-axis, 3-D arrangement of **1** based on 1-D

chains, (c) one-dimensional porous structure **1**, #: x-1, y-2, z+1;

Figure 2. (a) ORTEP figure of **2**, (b) 3-D arrangement of **2** based on 1-D chains, #: x+1/2, -y+3/2,

z+0.5;

Figure 3. (a) ORTEP figure of **3**, (b) 3-D arrangement of **3** based on 1-D chains, #: x-1, -y+1, -z;

Figure 4. Gas sorption isotherms of N_2 (77K) and CO_2 (195K) for **1d**;

Figure 5. Temperature dependence of $\chi_m T$ for coplexes **1-3**, the solid line represents the theoretical

values;
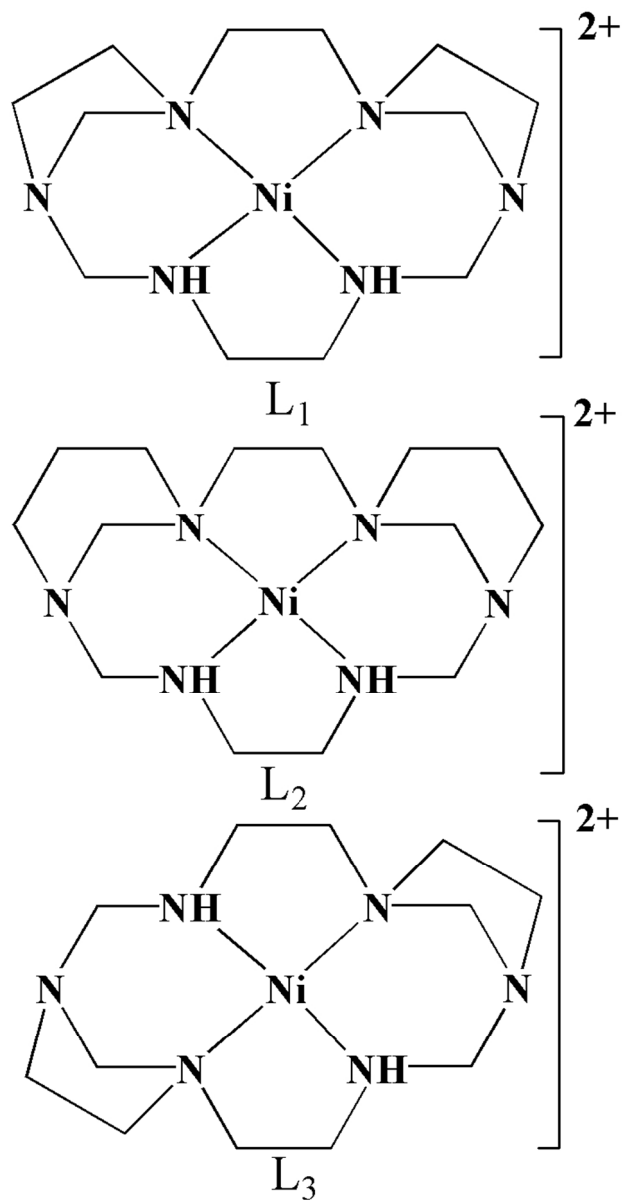
Scheme 1. Macrocyclic metallic tectons.
62x122mm (300 x 300 DPI)
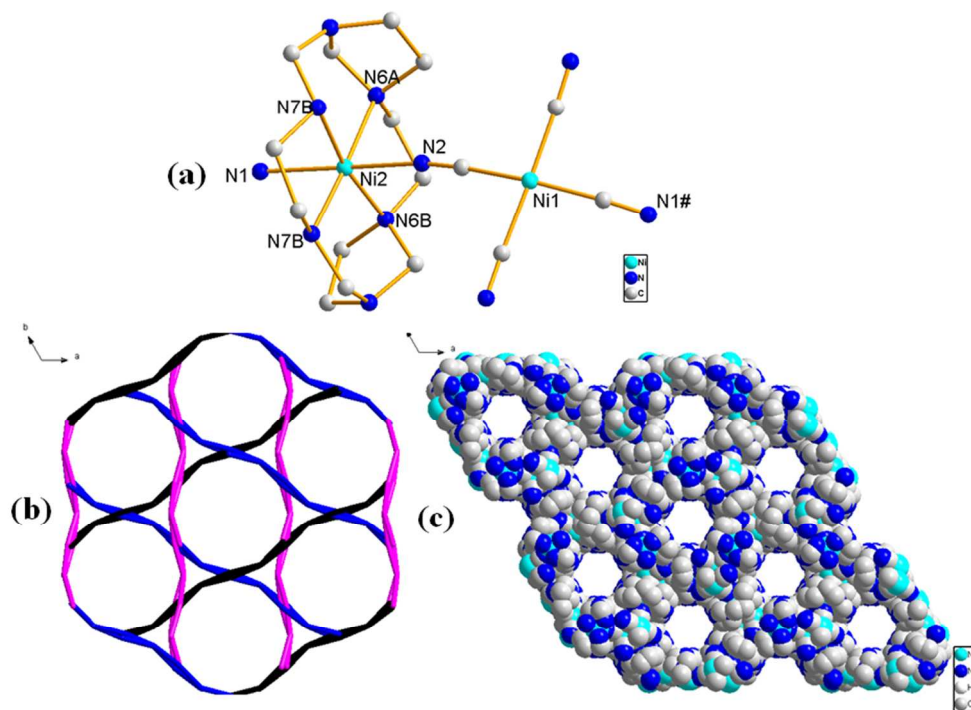
Figure 1. (a) ORTEP figure of 1, (b) view down the c-axis, 3-D arrangement of 1 based on 1-D chains, (c) one-dimensional porous structure 1, #: x-1, y-2, z+1;
254x184mm (300 x 300 DPI)
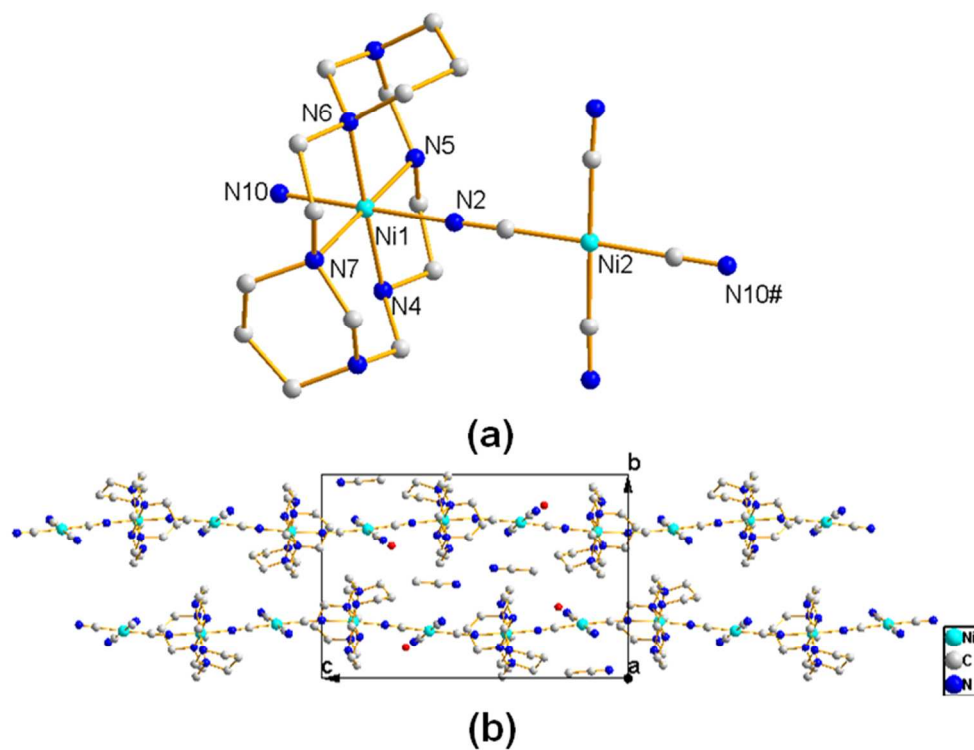
Figure 2. (a) ORTEP figure of 2, (b) 3-D arrangement of 2 based on 1-D chains, #: x+1/2, -y+3/2, z+0.5; 212x158mm (300 x 300 DPI)
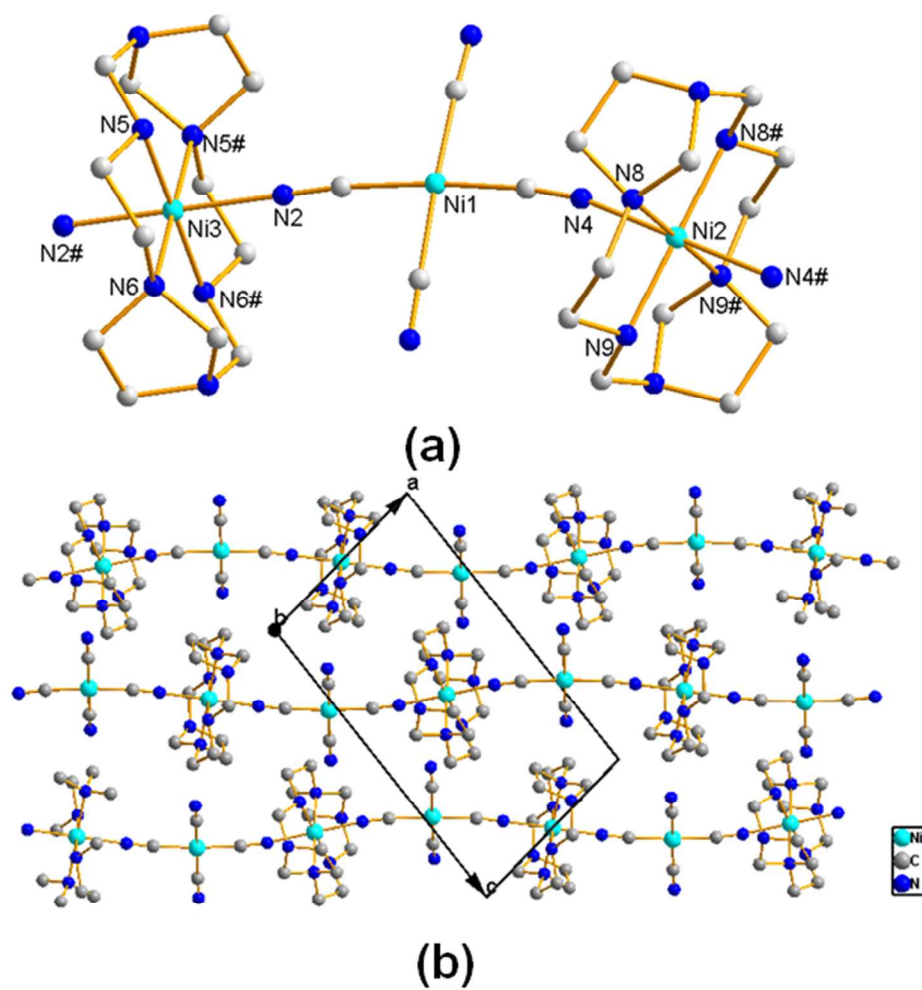
Figure 3. (a) ORTEP figure of 3, (b) 3-D arrangement of 3 based on 1-D chains, #: x-1, -y+1, -z; 176x177mm (300 x 300 DPI)
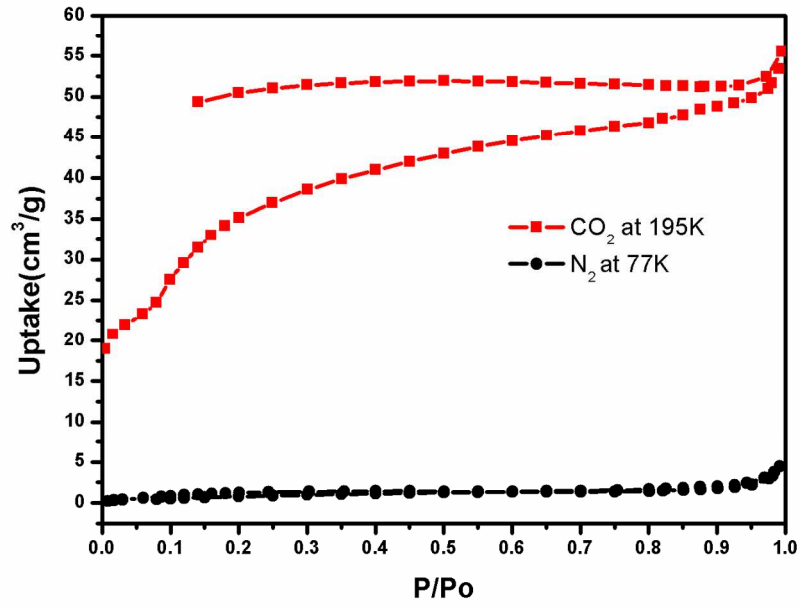
Figure 4. Gas sorption isotherms of N2 (77K) and CO2 (195K) for 1d;
297x209mm (150 x 150 DPI)

Figure 5. Temperature dependence of χmT for coplexes 1-3, the solid line represents the theoretical values; 297x209mm (150 x 150 DPI)